

An Integrated Backstepping and Sliding Mode Tracking Control Algorithm for Unmanned Underwater Vehicles

Bing Sun, Daqi Zhu, Weichong Li

Laboratory of Underwater Vehicles and Intelligent Systems
Shanghai Maritime University
Shanghai, China
email: zdq367@yahoo.com.cn

Abstract—In this paper, an integrated backstepping and sliding mode tracking control algorithm is developed for three-dimensional tracking control of unmanned underwater vehicles (UUV). The proposed control strategy combines with a kinematic controller and dynamic controller together. The kinematic controller integrates a bio-inspired model with the backstepping method while the dynamic controller uses robust sliding mode control. Unlike the traditional backstepping method suffering from the speed jump problem, the application of bio-inspired model can generate smooth and continuous velocity signal even in the large initial errors. Therefore, a smooth control signal can be obtained by dynamic controller without thruster control saturation. The effectiveness and efficiency of the proposed control strategy are demonstrated through simulations and comparison studies.

Keywords-Unmanned underwater vehicles, tracking control, backstepping, bio-inspired model.

I. INTRODUCTION

Unmanned underwater vehicles (UUV) have been widely used as a platform employed in risky missions such as oceanographic observations, bathymetric surveys, ocean floor analysis, military applications, recovery of lost man-made objects, etc [1]. This requires a more precise control behavior which has motivated an intensive research in the last decade. As a consequence, several different control approaches have been applied to the UUV motion control such as the adaptive control techniques [2-3], sliding-mode control [4-6], backstepping control algorithms [7-8], fuzzy-logic and neural network methods [9-12], etc.

The underwater vehicle dynamics is strongly coupled and highly nonlinear. In order to deal with the uncertain nonlinear parts in the underwater vehicle's dynamics, many researchers concentrated their interests on the applications of sliding mode control. Sliding mode method [4-5] is usually used for dynamic tracking control for the outstanding characteristic including insensitivity to parameter variations, and good rejection of disturbances. So sliding mode control is extraordinary suitable for robust tracking control of underwater vehicle. However, one major drawback of the sliding-mode approach is the high frequency of control action (chattering). To eliminate/reduce chattering, various methods have been proposed to reach a continuous robust control. For example, S. Serdar proposed a chattering-free sliding-mode

control method with an adaptive estimate term [6].

The backstepping control algorithms [7-8] is the commonly used approach for tracking control. However, the disadvantage for backstepping method is quite obvious. The velocity control law is directly related to the state errors, so large velocities will be generated in big initial error condition and sharp speed jump occurs while sudden tracking error happens. It means that the required acceleration and forces/moments exceed their control constraint even infinite values at the velocity jump points, which is practically impossible.

To resolve the impractical speed jump problem of large initial velocities resulted from the backstepping technique, some fuzzy control methods [9-10] and neural network control algorithms [11-12] are proposed. The fuzzy rules based tracking control approaches can solve the problem of large initial vehicle velocities, but it is very difficult to formulate the fuzzy rules, which are usually obtained by trial and error based human knowledge. As neural networks are characterized by flexibility and an aptitude for dealing with non-linear problems, they are envisaged to be beneficial when used on underwater vehicles. For examples, a neural network adaptive controller is proposed by Li [11] for autonomous diving control of an UUV using adaptive backstepping method when the smooth unknown dynamics of a vehicle is approximated by a neural network. Anyhow, the existing neural networks based tracking control algorithms for underwater vehicle require either on-line learning or off-line training procedures which could be computational complicated.

This paper focuses on the problem of speed jump and the thruster control constraints for UUV, and the a kinematics/dynamics cascaded control system integrating backstepping technology and sliding mode control with bio-inspired neural dynamics model (bio-inspired model) [13-14] is presented for three-dimensional (3D) tracking control of OUTLAND1000 UUV. Due to the shunting characteristics of bio-inspired model, the output of the bio-inspired model is bounded in a finite interval and smooth without any sharp jumps when inputs have sudden changes. In addition, the novel tracking controller proposed can meet on-line navigation of an UUV because no learning procedures are needed in the bio-inspired neural dynamics model.

This paper is organized as follows: In the second section, the basic kinematics and dynamics of the UUV. In the third section, an integrating backstepping and sliding mode tracking control algorithm based on bio-inspired model is presented. In

the fourth section thruster configuration and force allocation for OUTLAND1000 UUV are introduced. To illustrate effectiveness and efficiency of the proposed method, simulation examples are given in the fifth section. Finally, some concluding remarks are made.

II. BACKGROUND

In this section, two coordinate systems for UUV control are first briefly presented. Then the kinematic and dynamic model of UUV is provided. Finally the tracking control problem is briefly stated.

A. Kinematic model

In a three-dimensional (3D) Cartesian workspace shown in Fig. 1, two coordinate frame systems are defined: the inertial frame system $\{O - XYZ\}$ and the body-fixed frame system $\{O_0 - X_0 Y_0 Z_0\}$. The coordinate systems illustrated in Fig. 1 obey the right-hand rule and the Z-axis points to the downward.

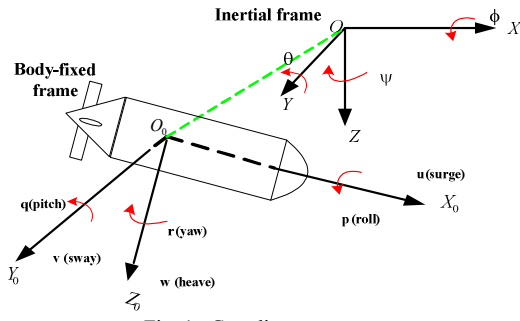


Fig. 1. Coordinate systems

The kinematic models are formulated as below. Let $\eta = [x \ y \ z \ \phi \ \theta \ \psi]^T$ be the generalized coordinates representing the position (x, y, z) and the orientation (ϕ, θ, ψ) with respect to the inertial frame and $q = [u \ v \ w \ p \ q \ r]^T$ be the translational velocities (u, v, w) and the rotational velocities (p, q, r) with respect to the body frame attached at the vehicle. Then, the kinematic model relating the body-fixed frame to the inertial frame can be expressed in a compact vector form as follows[24]:

$$\dot{\eta} = J(\eta)q \quad (1)$$

where $J \in R^{n \times n}$ is the spatial transformation matrix between the inertial frame and the UUV's body-fixed frame.

B. Dynamic model

The dynamic equation of UUV can be presented as a compact vector form [15]:

$$M\ddot{q} + C(q)\dot{q} + D(q)q + g(\eta) = \tau \quad (2)$$

where $M \in R^{n \times n}$ -inertia matrix including the added mass effects; $C \in R^{n \times n}$ -the matrix of Coriolis and centrifugal terms (including added mass caused by hydrodynamic effect); $D \in R^{n \times n}$ - the hydrodynamic damping matrix; $g \in R^n$ - gravity and buoyancy forces; $\tau \in R^n$ is the control forces and moments acting on the UUV centre of mass.

As mentioned earlier, the system dynamics are not exactly known. The system dynamics can be divided into two parts: estimated dynamics $\hat{\tau}$ and unknown dynamics $\tilde{\tau}$:

$$\tau = \hat{\tau} + \tilde{\tau} \quad (3)$$

where $\hat{\tau} = \hat{M}\ddot{q} + \hat{C}\dot{q} + \hat{D}q + \hat{g}$, $\tilde{\tau} = \tilde{M}\ddot{q} + \tilde{C}\dot{q} + \tilde{D}q + \tilde{g}$, $\hat{M}, \hat{C}, \hat{D}, \hat{g}$ are estimated terms, $\tilde{M}, \tilde{C}, \tilde{D}, \tilde{g}$ are the unknown terms.

In this paper, the mainly research focuses on the model of OUTLAND1000 UUV. The thruster configuration and force allocation of OUTLAND1000 UUV will be described in detail in section 4. It has only four degrees of freedom (DOF) (u, v, w, r) to conduct motion control, $p = q = 0$. So the simplified dynamic model in this paper's simulation is given as follows [16]:

$$(m - X_{\dot{u}})\dot{u} - mvr - X_u u - X_{uu}u|u| = \tau_x \quad (4)$$

$$(m - Y_{\dot{v}})\dot{v} - mur - Y_v v - Y_{vv}v|v| = \tau_y \quad (5)$$

$$(m - Z_{\dot{w}})\dot{w} - Z_w w - Z_{ww}w|w| = \tau_z \quad (6)$$

$$(I_z - N_r)\dot{r} + muv - mur - N_r r - N_{rr}r|r| = \tau_N \quad (7)$$

where $X_{\dot{u}}, Y_{\dot{v}}, Z_{\dot{w}}, N_r$ is the added mass effect, X_u, Y_v, Z_w, N_r is the linear drag and $X_{uu}, Y_{vv}, Z_{ww}, N_{rr}$ is the quadratic drag.

C. Tracking control problem

The UUV is usually required to move at a low forward speed and a low rotational speed when it executes investigation tasks. This needs a precious tracking control. Consider that the UUV's major movement is in four degrees of freedom (DOF): surge, sway, heave, yaw, so in this paper, only the four DOF tracking control problem is represented. The controller design problem can be described as follows. The desired state of UUV is defined as

$$\eta_d = [x_d \ y_d \ z_d \ \psi_d]^T \quad (8)$$

where $\eta_d = [x_d \ y_d \ z_d \ \psi_d]^T$ is the desired state of UUV in the inertial frame, (x_d, y_d, z_d) is coordinate of desired path in the inertial frame, ψ_d is the counter-clockwise rotation angle of UUV along the Z-axis.

The desired forward and angular velocities can be deduced by

$$\begin{aligned} u_d &= \dot{x}_d \cos \psi_d + \dot{y}_d \sin \psi_d \\ v_d &= \dot{x}_d (-\sin \psi_d) + \dot{y}_d \cos \psi_d \\ w_d &= \dot{z}_d \\ r_d &= \dot{\psi}_d = \frac{\dot{x}_d \dot{y}_d - \dot{y}_d \dot{x}_d}{\dot{x}_d^2 + \dot{y}_d^2} \end{aligned} \quad (9)$$

The actual state of UUV is represented by $\eta = [x \ y \ z \ \psi]^T$, $q = [u \ v \ w \ r]^T$. As the objective of the path tracking controllers is to make UUV follow the known path by controlling the velocity and angular velocities,

so the tracking error $\mathbf{e} = \boldsymbol{\eta}_d - \boldsymbol{\eta} = [e_x \ e_y \ e_z \ e_\psi]^T$ converges to zero. Here \mathbf{e} is the tracking error in the inertial frame. A detailed model of tracking control problem is given in Fig. 2.

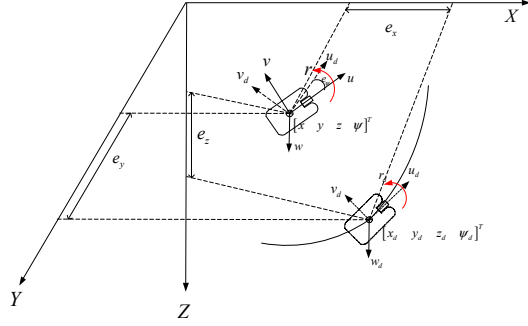


Fig. 2. Tracking control problem

III. CONTROL ALGORITHMS

The basic control architecture of the system is illustrated in Fig. 3. The design of the hybrid control strategy consists of two parts: (1). an outer loop virtual velocity controller by using position and orientation state errors; (2). an inner loop sliding-mode controller by using velocity state vector.

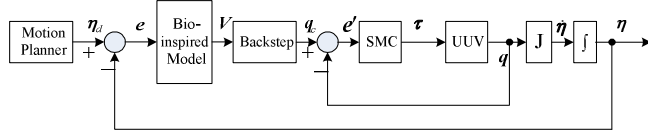


Fig. 3. The cascaded controller of UUV

A. Virtual velocity controller

Backstepping method for nonholonomic mobile robot has been designed a lot for velocity tracking [12-13]. But the UUV in this study is a holonomic system, so the backstepping control law for the mobile robot is not fit for this control system. For this reason, a new backstepping control law is designed for UUV and makes it possible to follow a given reference posture with stability.

The virtual velocity controller based on the backstepping approach can be defined as:

$$\mathbf{q}_c = \begin{bmatrix} u_c \\ v_c \\ w_c \\ r_c \end{bmatrix} = \begin{bmatrix} k(e_x \cos \psi + e_y \sin \psi) + (u_d \cos e_\psi - v_d \sin e_\psi) \\ k(-e_x \sin \psi + e_y \cos \psi) + (u_d \sin e_\psi + v_d \cos e_\psi) \\ w_d + k_z e_z \\ r_d + k_\psi e_\psi \end{bmatrix} \quad (10)$$

where k, k_z, k_ψ are constant coefficients, $\mathbf{q}_d = [u_d \ v_d \ w_d \ r_d]^T$ is the desired velocity in the body-fixed frame, $u_d \cos e_\psi - v_d \sin e_\psi$, $u_d \sin e_\psi + v_d \cos e_\psi$ represents the desired velocity frame transformed to the actual velocity frame seen in Fig. 2.

B. Bio-inspired velocity controller

In-depth analysis of (10), the virtual speed can be found directly related to the tracking errors. In order to resolve the speed jump and control constraint problem, a bio-inspired model is added in the controller to design the virtual velocity.

Bio-inspired neural dynamics model was first developed by Grossberg [17]. It can describe an on-line adaptive behavior of individuals. It was originally derived based on the membrane model proposed by Hodgkin and Huxley [18] for a patch of membrane using electrical elements. The dynamics of voltage across the membrane V_m can be described in the membrane model using state equation technique as

$$C_m \frac{dV_m}{dt} = -(E_p + V_m)g_p + (E_{Na} - V_m)g_{Na} - (E_k + V_m)g_k \quad (11)$$

where C_m is the membrane capacitance. The parameters E_k , E_{Na} and E_p are the Nernst potentials for potassium ions, sodium ions, and passive leak current in the membrane, respectively. g_k , g_p and g_{Na} are the conductance of potassium, sodium and the passive channels are functions of input signals that vary with time.

To simplify the equation, a shunting equation is obtained as

$$\dot{V} = -AV + (B - V)S(t)^+ - (D + V)S(t)^- \quad (12)$$

where V is the neural activity of the neuron. Parameters A, B and D are respectively the passive decay rate, the upper and lower bounds of the neural activity. The variables S^+ and S^- represent the excitatory and inhibitory input, respectively. The shunting dynamic of an individual neuron can be modeled by this equation. The neuron dynamics are restricted to a bounded interval $[-D, B]$ and an automatic gain control. So we can infer the shunting equation to the following form

$$\dot{V}_i = -AV_i + (B - V_i)f(e_i) - (D + V_i)g(e_i) \quad (13)$$

where $f(e_i) = \max(e_i, 0)$, $g(e_i) = \max(-e_i, 0)$, A, B, D are positive constants. For a system with appropriate chosen inputs, various desirable functional properties such as competitive, short memory, upper bound and lower bound can be derived from the model. The systems output V is guaranteed to stay in a region $[-D, B]$ for any excitatory and inhibitory inputs.

So the proposed virtual velocity controller can be given as

$$\mathbf{q}_c = \begin{bmatrix} u_c \\ v_c \\ w_c \\ r_c \end{bmatrix} = \begin{bmatrix} k(V_x \cos \psi + V_y \sin \psi) + (u_d \cos e_\psi - v_d \sin e_\psi) \\ k(-V_x \sin \psi + V_y \cos \psi) + (u_d \sin e_\psi + v_d \cos e_\psi) \\ w_d + k_z V_z \\ r_d + k_\psi V_\psi \end{bmatrix} \quad (14)$$

where k, k_z, k_ψ are the same parameters of (13). Due to the shunting characteristics of bio-inspired model, the output of the bio-inspired model is bounded in a finite interval and smooth without any sharp jumps when inputs have sudden changes. So the controller performance is significantly improved.

C. The adaptive sliding-mode controller

After the velocity controller generates the virtual velocity of the underwater vehicles, a sliding-mode controller is used to generate the control forces and moments $\boldsymbol{\tau} = [\tau_x \ \tau_y \ \tau_z \ \tau_n]^T$.

Then the control inputs τ will be applied to the UUV dynamic model to produce the actual velocity in surge, sway, heave and yaw ($\mathbf{q} = [u \ v \ w \ r]^T$) in the body-fixed frame respectively. So it will be easy to get the actual underwater vehicle's states ($\eta = [x \ y \ z \ \psi]^T$) in the inertial frame by $\dot{\eta} = J\mathbf{q}$.

As a rule, sliding-mode control can be divided into two parts. First, define a sliding manifold s . Second, find a control law to move toward the sliding manifold. The sliding manifold is defined as[8]:

$$s = \dot{e}_c + 2\Lambda e_c + \Lambda^2 \int e_c \quad (15)$$

where $e_c = \mathbf{q}_c - \mathbf{q}$ is the velocity error between the virtual velocity and the actual velocity, Λ represents a strictly positive constant, s is a 4×1 vector. Derivation of (15), then

$$\dot{s} = \ddot{e}_c + 2\Lambda \dot{e}_c + \Lambda^2 e_c = \ddot{e}_c + 2\Lambda(\dot{\mathbf{q}}_c - \dot{\mathbf{q}}) + \Lambda^2 e_c \quad (16)$$

When the system is operating on the sliding surface, (11) equals zero, i.e.

$$\dot{s} = \ddot{e}_c + 2\Lambda \dot{e}_c + \Lambda^2 e_c = \ddot{e}_c + 2\Lambda(\dot{\mathbf{q}}_c - \dot{\mathbf{q}}) + \Lambda^2 e_c = 0 \quad (17)$$

Substituting (2) into (17), then

$$\ddot{e}_c + 2\Lambda(\dot{\mathbf{q}}_c - M^{-1}(\tau - C\mathbf{q} - D\mathbf{q} - g)) + \Lambda^2 e_c = 0 \quad (18)$$

So the equivalent control law can be concluded as

$$\tau_{eq} = \hat{M}(\dot{\mathbf{q}}_c + \frac{\ddot{e}_c}{2\Lambda} + \frac{\Lambda}{2} e_c) + \hat{C}\mathbf{q} + \hat{D}\mathbf{q} + \hat{g} \quad (19)$$

where $\hat{M}, \hat{C}, \hat{D}, \hat{g}$ are estimated terms. Considering the difficulty of computing \ddot{e}_c in (19), a feedback control input of acceleration error is introduced

$$\ddot{e}_c = -k\dot{e}_c \quad (20)$$

where k is a constant scalar representing the strictly positive constant that determines the rate of acceleration error.

The conventional sliding-mode can be designed as

$$\tau = \tau_{eq} + k \operatorname{sgn}(s) \quad (21)$$

To eliminate chattering problem caused by the discontinuous term, an adaptive term [8] is added in the control law to replace the switching term

$$\tau_{ad} = \tilde{\tau}_{est} + (K + \frac{\hat{C}}{2\Lambda})s \quad (22)$$

where $\tilde{\tau}_{est}$ is an adaptive term that estimates the lumped uncertainty vector defined in (3), K is also a constant scalar representing the strictly positive constant related to the convergence rate of the controller. The estimation of the lumped uncertainty vector is proposed to follow:

$$\dot{\tilde{\tau}}_{est} = \Gamma s \quad (23)$$

where Γ represent the strictly positive constant that determines the rate of adaption.

The total control law can be defined as

$$\tau = \tau_{eq} + \tau_{ad} = \tau_{eq} + \tilde{\tau}_{est} + (K + \frac{\hat{C}}{2\Lambda})s \quad (24)$$

IV. FORMULATION OF THE CONTROL ALLOCATION PROBLEM

The OUTLAND1000 is used to demonstrate the performance of the proposed bio-inspired cascaded tracking control approach. It has four fixed direction thrusters; three horizontal thrusters denoted as $HT^i, i \in [1, 3]$, and one vertical thruster denoted as VT^1 . The OUTLAND1000 and the thruster's configuration enables direct control of surge, yaw and heave, as indicated in Fig. 4, 5.

In this paper the four degree motion control is discussed. Each thruster exerts thrust (force) \mathbf{F} and torque \mathbf{Q} . The position vector $\mathbf{r} = [r_x \ r_y \ r_z]^T$ determines the position of the point of attack of the force \mathbf{F} . The orientation of the thruster is defined by the unit vector $\mathbf{e} = [e_x \ e_y \ e_z]^T$. The force \mathbf{F} also generates the moment $\mathbf{Q} = \mathbf{r} \times \mathbf{F}$. The vector of forces and moments can be written as [19]:

$$F_i = k_1 n_i^2 = k u_i^2, n_i = k_2 u_i, Q_i = r_i \times k u_i^2, i = 1, 2, 3, 4 \quad (25)$$

where $\lambda = k_1 k_2$ is the thruster motor control parameter, u_i is the control voltage of i th thruster, n_i is the rotational speed of i th thruster.



Fig. 4 OUTLAND1000

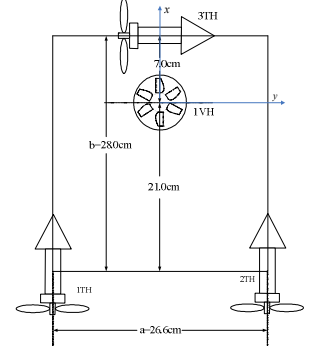


Fig. 5 Configuration of the thrusters

The total vector of propulsion forces and moments τ in the horizontal plane are considered:

$$\tau = \begin{bmatrix} \tau_x \\ \tau_y \\ \tau_z \\ \tau_N \end{bmatrix} = \begin{bmatrix} \lambda & \lambda & 0 & 0 \\ 0 & 0 & \lambda & 0 \\ 0 & 0 & 0 & \lambda \\ a\lambda/2 & -a\lambda/2 & (b-21)\lambda & 0 \end{bmatrix} \begin{bmatrix} u_1^2 \\ u_2^2 \\ u_3^2 \\ u_4^2 \end{bmatrix} = B \cdot u \quad (26)$$

where τ are represented as the motions of surge, sway, heave and yaw respectively, and $a\lambda/2 = 13.3\lambda$, $(b-21)\lambda = 7\lambda$ (from Fig. 5). Each component of the control vector is limited by constraint:

$$-u_m \leq u_i \leq u_m, -n_m \leq n_i \leq n_m, i = 1, 2, 3, 4 \quad (27)$$

where u_m is the thruster maximum control variable, n_m is the thruster maximum rotational speed. From (25) and (26):

$$\tau_{xm} = 2F_m = 2\lambda u_m^2 \Rightarrow \lambda = 2\tau_{ym} / u_m^2 \quad (28)$$

$$\tau_{ym} = F_m = \lambda u_m^2 \Rightarrow \lambda = \tau_{ym} / u_m^2 \quad (29)$$

$$\tau_{zm} = F_m = \lambda u_m^2 \Rightarrow \lambda = \tau_{zm} / u_m^2 \quad (30)$$

$$\tau_{Nm} = a\lambda u_m^2 / 2 + (b-21)\lambda u_m^2 = 20.3\lambda u_m^2 \Rightarrow 20.3\lambda = \tau_{Nm} / u_m^2 \quad (31)$$

Finally, the general constrained control allocation problem for the OUTLAND1000 can be formulated as: For given normalized $\bar{\tau}$, find \bar{u} feasibility such that

$$\bar{\tau} = \bar{B} \cdot \bar{u} \quad (32)$$

where $-1 \leq \bar{u} = [\frac{u_1}{u_m} \quad \frac{u_2}{u_m} \quad \frac{u_3}{u_m} \quad \frac{u_4}{u_m}]^T \leq 1$, $-1 \leq \bar{\tau} \leq 1$,

$$\bar{\tau} = [\frac{\tau_x}{\tau_{xm}} \quad \frac{\tau_y}{\tau_{ym}} \quad \frac{\tau_z}{\tau_{zm}} \quad \frac{\tau_n}{\tau_{nm}}]^T, \quad \bar{B} = \begin{bmatrix} 1/2 & 1/2 & 0 & 0 \\ 0 & 0 & 1 & 0 \\ 0 & 0 & 0 & 1 \\ 0.655 & -0.655 & 0.345 & 0 \end{bmatrix}.$$

V. SIMULATION

In this paper, the two methods were simulated for tracking control problem: the proposed backstepping method and the bio-inspired method. The backstepping method given in (10) was used as a case study to illustrate the performance of the proposed control strategies. From the simulation results, the proposed controller can reach a robust control while the speed jump and thruster saturation problem can be solved successfully.

The hydrodynamic parameter of OUTLAND1000 UUV is given in Table I by estimation through the comparison of the similar UUV model [16]. To reflect uncertainties of the vehicle dynamics, 20% model inaccuracies were incorporated into the controller's dynamic model. It means that in the following simulations, the parameters in Table I will be set as the actual value, while the estimated value is 80% of the actual value. The parameter setting of the cascaded controller is shown in Table II.

Table I. Hydrodynamic Parameters of OUTLAND1000 UUV

$X_u = 34$	$X_u = 6$	$X_{uu} = 18$
$Y_v = 75$	$Y_v = 10$	$Y_{vv} = 4$
$Z_w = 33$	$Z_w = 7$	$Z_{ww} = 4$
$N_r = 62$	$N_r = 14$	$N_r = 14$

A typical case to track a spiral line is studied. The UUV starts at Posture $(0, 0, 1, 0)$, while the desired initial robot posture is $(0, -2, 0, 0)$. Thus the initial posture error is $(0, -2, -1, 0)$. Time varies from 0 to 20s. The desired state of UUV is $x_d(t) = 2\sin(0.5t)$, $y_d(t) = -2\cos(0.5t)$, $z_d(t) = 0.1t$, $\psi_d(t) = 0.5t$. The parameter setting of the hybrid controller is shown in Table II.

Table II. Controller Parameters

k_c	Γ	K	Λ	k	k_z	k_ψ	A	B	D
10	5	100	3	2	2	5	2	1	1

Fig. 6 ~ Fig. 8 shows the simulation results of the spiral line tracking. The red solid lines indicate the backstepping method results, and the blue solid lines are the bio-inspired method results. Fig. 6 gives the desired trajectory and tracking control results of backstepping method and bio-inspired method on the same condition. Fig. 7 shows the virtual

velocity q_c by the backstepping method and bio-inspired method. The normalized thruster control variable \bar{u} of trajectory tracking is shown in Fig. 8. Table III is the maximum normalized control variable of each thruster.

In the simulation results of trajectory tracking in Fig. 6, it seems that for both two methods, the UUV can drive to reach and stay on the trajectory in quick response. In Fig. 7, for the virtual velocity controller based on the backstepping approach (non-biological inspired), this virtual velocity q_c occurs the sharp speed jumps when tracking errors change suddenly at initial time. For example the virtual sway speed of the backstepping method jumps to -4m/s , but the bio-inspired method is limited in the range of $-0.5\text{m/s} \sim 0\text{ m/s}$ in Fig. 7.

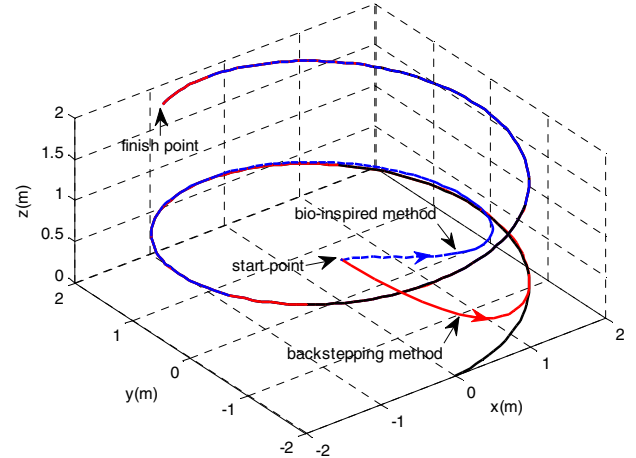


Fig. 6. Systems trajectories using bio-inspired model and the backstepping method

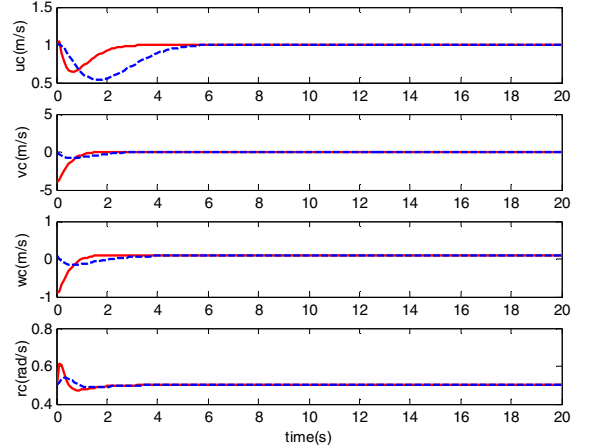


Fig. 7. Virtual velocity using bio-inspired model (dotted line) and the backstepping method (solid line)

In order to catch up the virtual velocities, the UUV accelerates both linear and angular velocities. So the UUV needs to generate quite large forces/momenta to track the virtual velocity q_c . It means that the required acceleration and forces/momenta may exceed their control constraint values at the velocity jump points. In order to achieve such large speed, it can be seen that the maximum normalized thruster control variable of \bar{u}_3 is -5.6880 and the other maximum normalized

thruster control variable are also greater than the limitation output ($-1 \leq \bar{u} \leq 1$) which is practically impossible. In addition, the control variable needs more time to adjust the overshoot process. By contrast, for the bio-inspired tracking control method, no any control value exceeds their maximum control values, and all control forces limited in the thruster control saturation point. This proves the efficiency of the proposed cascaded tracking method.

Table III. Maximum normalized thruster control variable

Algorithm	\bar{u}_1	\bar{u}_2	\bar{u}_3	\bar{u}_4
Backstepping method	2.4953	-1.8335	-5.6880	-2.3782
Bio-inspired method	0.9055	-0.6122	-0.5290	-0.4728

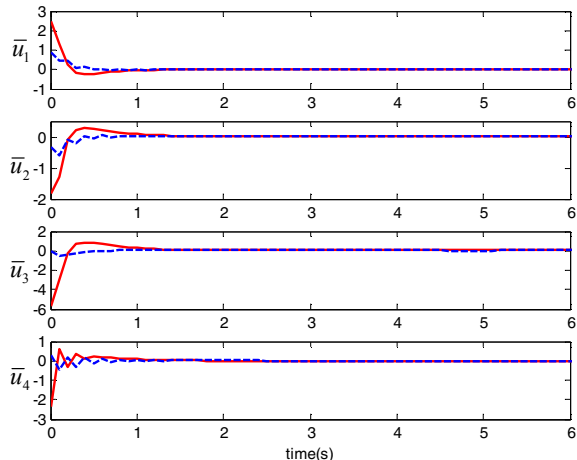


Fig. 8. Thruster forces using bio-inspired model (dotted line) and the backstepping method (solid line)

VI. CONCLUSION

Background information about tracking control of unmanned underwater vehicles is firstly established in the paper. Then an integrated backstepping and sliding mode tracking control algorithm is proposed for three-dimensional tracking control problem. In the control system, there exist two closed loop systems: inner loop ensures the velocity tracking and the outer loop ensures the position and orientation tracking. In the traditional backstepping method, it always suffers from the sharp speed jump problem which will cause thruster saturation. Because of the smooth and bounded response properties, the proposed velocity controller uses the bio-inspired model to eliminate or inhibit the sharp speed jumps. From the simulation results, it is clearly to see bio-inspired method reduces the thrust output obviously without significant performance loss while the conventional backstepping method may cause thruster saturation.

In the dynamic controller, the sliding mode control method uses an adaptive term to compensate the nonlinear uncertainties part and the disturbance of the underwater vehicles dynamics. Simulation results showed that the designed controller performs well with stability and

robustness. On the other hand, ocean currents should be added to the outside interference. This warrants further research.

ACKNOWLEDGMENT

This project is supported by the National Natural Science Foundation of China (51075257) and the Creative Activity Plan for Science and Technology Commission of Shanghai (10550502700), the Project of Excellent Academic Leaders of Shanghai (11XD1402500) and the Yangtze River Delta Region scientific and technological project (10595812700).

REFERENCES

- [1] J. Yuh, Design and Control of Autonomous Underwater Robots: A Survey, *Autonomous Robots*, vol. 8, no. 1, pp. 7-24, Jan. 2000.
- [2] G. Antonelli, F. Caccavaleet, and S. Chiaverini, Adaptive tracking control of underwater vehicle-manipulator systems based on the virtual decomposition approach, *IEEE Trans. Robot. Autom.*, vol. 20, no. 3, pp. 594-602, Jun. 2004.
- [3] D. A. Smallwood and L. L. Whitcomb, Model-based dynamic positioning of underwater robotic vehicles: Theory and experiment, *IEEE J. Ocean. Eng.*, vol. 29, no. 1, pp. 169-186, Jan. 2004.
- [4] V. Sankaranarayanan and A. D. Mahindrakar, Control of a Class of Underactuated Mechanical Systems Using Sliding Modes, *IEEE Trans. Robot.*, vol. 25, no. 2, pp. 459-467, Apr. 2009.
- [5] T. Nguyen, J. Leavitt, F. Jabbari, and J. E. Bobrow, Accurate sliding-mode control of pneumatic systems using low-cost solenoid valves, *IEEE/ASME Trans. Mechatronics*, vol. 12, no. 2, pp. 216-219, Apr. 2007.
- [6] S. Soylu, B. J. Buckham, R. P. Podhorodeski, A chattering-free sliding-mode controller for underwater vehicles with fault-tolerant infinity-norm thrust allocation, *Ocean Engineering*, vol. 35, no. 16, pp. 1647-1659, Nov. 2008.
- [7] L. Lapierre and B. Jouvencel, Robust Nonlinear Path-Following Control of an AUV, *IEEE J. Oceanic Eng.*, vol. 33, no. 2, pp. 89-102, Apr. 2008.
- [8] R. Fierro and F. L. Lewis, Control of a nonholonomic mobile robot: Backstepping kinematics into dynamics, *J. Robot. Syst.*, vol. 14, no. 3, pp. 149-163, 1997.
- [9] K. Ishaque, S. S. Abdullah, and S. M. Ayob, A simplified approach to design fuzzy logic controller for an underwater vehicle, *Ocean Engineering*, vol. 38, pp. 271-284, Jan. 2011.
- [10] G. Antonelli, S. Chiaverini, and G. Fusco, A fuzzy-logic-based approach for mobile robot path tracking, *IEEE Trans. Fuzzy Syst.*, vol. 15, no. 2, pp. 211-221, Apr. 2007.
- [11] J. H. Li, P. M. Lee, and B. H. Jun, A neural network adaptive controller for autonomous diving control of an autonomous underwater vehicle, *International Journal of Control Automation and Systems*, vol. 2, no. 3, pp. 374-383, Sep. 2004.
- [12] V. S. Kodogiannis, Neuro-control of unmanned underwater vehicles, *Int J of Systems Sc.*, vol. 37, no. 3, pp. 149-162, Feb. 2006.
- [13] C. Luo and S. X. Yang, A bio-inspired neural network for real-time concurrent map building and complete coverage robot navigation in unknown environment, *IEEE Trans. Neural Netw.*, vol. 19, no. 7, pp. 1279-1298, Jul. 2008.
- [14] S. X. Yang and C. Luo, A neural network approach to complete coverage path planning, *IEEE Trans Syst Man Cybern B*, vol. 34, no. 1, pp. 718-725, Feb. 2004.
- [15] T. I. Fossen, *Guidance and Control of Ocean Vehicles*, Wiley, New York, 1994.
- [16] D. Steinke, Design and simulation of a Kalman filter for ROV navigation, Master Thesis, University of Victoria, 2003.
- [17] S. Grossberg, Nonlinear neural networks: Principles, mechanisms, and architectures, *Neural Networks*, vol. 1, no. 1, pp. 17-61, 1988.
- [18] A. L. Hodgkin and A. F. Huxley, A quantitative description of membrane current and its application to conduction and excitation in nerve, *J. Physiol.*, vol. 117, no. 4, pp. 500-544, 1952.
- [19] A.J. Sorensen and Y.N. Smogeli, Torque and power control of electrically driven marine propellers, *Control Engineering Practice*, vol. 17, no. 10, pp. Sep. 1053-1064, 2009.